Localization of Ca^{2+} at the Plasma Membrane of Bullfrog Myocardial Cells

R. Meyer, M. Schmitz, W. Stockem,

Institut für Cytologie, Universität Bonn, Ulrich-Haberland-Str. 61 A, D-5300 Bonn

and H. G. Haas

Institut für Physiologie II, Universität Bonn, Wilhelmstr. 31, D-5300 Bonn

Z. Naturforsch. **37 c**, 1180–1190 (1982); received August 12, 1982

Bullfrog Myocardial Sarcolemma, Histochemistry, Cryofixation, X-ray Microanalysis, Ca^{2+}-Binding Sites

Cellular distribution and localization of Ca^{2+} in bullfrog myocardial cells was investigated on the light and electron microscopical level using different preparation procedures. Fixation and dehydration in glutaraldehyde and ethanol solutions containing increased amounts of Ca^{2+} (5–25 mM) cause the formation of numerous electron-dense deposits at the external face of the sarcolemma. X-ray microanalysis demonstrates that the deposits are mainly composed of calcium. Similar results were obtained in cryopreparations by quick-freezing of fresh myocardial tissue. Granules with a diameter of 16.6 nm, which clearly exceed all other cell constituents in contrast, are found at the entire myocardial cell surface. Besides an increased amount of calcium the granules contain potassium and phosphorus. Fluorescence microscopy on single cells obtained from bullfrog atrium by treatment with digestive enzymes and stained with chlorotetracycline (CTC) as a fluorescent probe for membrane-bound Ca^{2+} clearly support the observations made on the fine structural level. A strong fluorescence signal depending on the CTC- and Ca^{2+}-concentration of the incubation medium is observed at the sarcolemma and can be inhibited by addition of La^{3+}.

The results of the present investigation suggest that the surface coat of the sarcolemma of myocardial cells represents an important compartment for accumulation and release of external Ca^{2+}. The external lamina which partly covers the surface of myocardial cells seems not to be involved in the Ca^{2+} exchange.

Introduction

Contractile activity of heart muscle cells depends on Ca^{2+} derived from extra- and intracellular sources. One hundred years ago Ringer was the first to demonstrate that the contractile force of isolated heart tissue rapidly declines in Ca^{2+}-free solution, *i.e.* easily exchangeable Ca^{2+} is involved in the initiation of cardiac muscle contraction. In the past two decades, the existence of different rapidly and slowly exchangeable kinetic compartments for Ca^{2+} has been established [1–3]. A more rapidly exchangeable compartment participates in contractile activation and is inhibited by La^{3+} [3]. Experiments using the pyroantimonate method delivered evidence for the localization of Ca^{2+} along the sarcolemma [4]. Both, biochemical studies on isolated plasma membranes of heart tissue [5–8] and zeta potential measurements [9] confirmed the concept of a Ca^{2+}-binding function of the sarcolemma and a competition of Ca^{2+} with other cations for a common binding site [5, 10]. In addition to the extracellular calcium as a source of activator calcium, a Ca^{2+}-induced Ca^{2+}-release from intracellular compartments such as the sarcoplasmic reticulum and mitochondria is also regarded to take part in control of heart muscle contraction [11].

While many investigations supply indirect evidence for participation of the sarcolemma in Ca^{2+}-regulation, a direct demonstration of Ca^{2+}-binding sites or accumulated Ca^{2+}-ions at the myocardial plasma membrane is still lacking. In the present investigation amphibian heart tissue was used for the demonstration of Ca^{2+} at the cell surface, because the contractile response of this tissue is almost exclusively controlled by extracellular Ca^{2+} [11]. In a series of experiments we used the technique of Oschman and Wall [12] for the decoration of Ca^{2+}-binding sites and localized *in vivo*-bound Ca^{2+} on the electron and light microscopical level by cryopreparations in connection with X-ray microanalysis and chlorotetracycline (CTC)-fluorescence in living cells, respectively. As both, the sarcolemma and the

Reprint requests to Prof. Dr. W. Stockem, Institut für Cytologie, Ulrich-Haberland-Str. 61 A, D-5300 Bonn, FRG.

0341-0382/82/1100-1180 $ 01.30/0

external lamina [13] are possible sites for Ca^{2+}-storage, a morphometrical evaluation was carried out to calculate the surface ratio of the two constituents.

Materials and Methods

For morphometrical and histochemical investigations muscle strips dissected from bullfrog (*Rana catesbeiana*) auricles in Ringer's solution (111 mM NaCl, 5.4 mM KCl, 2 mM $CaCl_2$, 1.8 mM $KHCO_3$) were placed in dishes with paraffin-covered bottom and attached to the ground with small needles to avoid contraction during fixation and dehydration.

Muscle strips used for morphometry were fixed according to Dalton [14] and Wohlfarth-Bottermann [15]:

Fixation with 2% OsO_4 and 1% $K_2Cr_2O_7$ in 0.15 M PIPES-buffer (pH 7.2) for 1 h; washing for 2 h in 0.15 M PIPES-buffer; postfixation with 1% OsO_4 in 0.15 M PIPES-buffer for 1 h; washing in 0.15 M PIPES-buffer for 1 h; dehydration in a graded series of ethanols; embedding in Spurr's low viscosity epoxy resin [16].

Muscle strips used for histochemistry were fixed with Ca^{2+}-containing fixation solutions according to Oschman and Wall [12]:

1. Fixation with 2.5% glutaraldehyde in 0.05 M cacodylate-buffer (pH 7.2) for 1 h, or
2. 2.5% glutaraldehyde in 0.15 M PIPES-buffer (pH 7.2) for 1 h.

The fixation media were removed by washing in the corresponding buffer for 2 h. Specimens were dehydrated and embedded as described above. All solutions up to 90% ethanol contained different concentrations of $CaCl_2$, *i.e.* 5 mM, 10 mM or 25 mM. Control tissue was prepared without $CaCl_2$ or with 2 mM EGTA instead of $CaCl_2$.

For freeze-drying single trabeculae (diameter about 100 µm) were positioned in aluminium sandwiches (Fig. 1), mounted at the tip of small projectiles and shut by means of a crossbow-like apparatus into a tube filled with liquid propane [17] cooled with liquid nitrogen. The specimens were then transferred to liquid nitrogen, removed from the projectile, and stored after opening of the sandwich in a cooled-container at − 190 °C for freeze-drying and embedding. Specimens were dried in a Leybold-Heraeus freeze-drying unit (GT 1) for three days at − 110 °C and a pressure below 10^{-4} mbar. Temperature was then slowly raised to − 10 °C without increase of pressure, and Spurr's low viscosity epoxy resin was directly conducted from an evacuated prechamber into the storage container. Specimens were kept under these conditions (− 10 °C, 10^{-4} mbar) until infiltration with resin was completed and were then conventionally embedded.

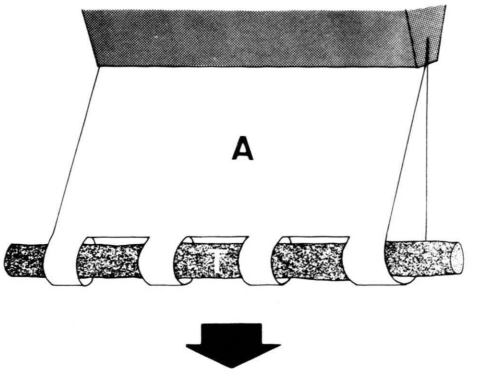

Fig. 1. Schematic drawing of the projectile with a mounted specimen used for cryofixation. A fenestrated aluminium sheet (A) is wrapped around a single trabeculum (T). The arrow indicates the direction of the projectile as shot into the propane.

Ultrathin sections cut with LKB-ultrotomes were usually stained with 1% uranyl acetate in 70% ethanol at 4 °C for 30 min. Some sections (for histochemical preparations) were stained with 3% uranyl acetate in 70% ethanol at room temperature for 1 min. Sections for X-ray microanalysis were cut without floating on water, *i.e.* dry to avoid solvation of ions, and remained always unstained. Sections were observed with a Philips 200 electron microscope at 40 kV or 60 kV or with a Philips 301 electron microscope at 80 kV. X-ray microanalysis was carried out with a Philips 300 electron microscope at 80 kV equipped with a STEM unit and an EDAX-microprobe analyser. X-ray spectra were detected in STEM-mode.

For fluorescence microscopy small pieces of tissue were disaggregated into single cells by incubation in Ringer's solution containing low concentrations of Ca^{2+} (*i.e.* 10^{-5} M free Ca^{2+}), 0.1% collagenase and 0.1% trypsin [18]. Single living cells were attached to microscopical slides coated with poly-l-lysine [19] and washed with Ringer's solution con-

taining 10^{-5} M Ca^{2+}. Ringer's solution was then replaced by the same solution containing in addition 250 µM chlorotetracycline (CTC, Serva, Heidelberg, FRG), *i.e.* a fluorescent dye for membrane-bound Ca^{2+} [20]. After staining for about 5 min the Ca^{2+}-concentration was raised to the usual level of 2 mM. In some experiments 200 µm La^{3+} as an additive to Ringer's solution without $KHCO_3$ was applied.

Fluorescence and bright field microscopy were carried out with Zeiss Photomikroskop I equipped with Zeiss Plan-Neofluar objectives. An image intensification system (TV-compact camera K5B, Siemens) allowed the application of excitation light at low intensities (exciter filter: 405 nm; cut-off filter: 460 nm). The cells were photographed from pictures displayed on a TV-screen.

Results

1. Morphometry

Two separate systems of external laminas (Fig. 2b, EL_1 and EL_2) encircling myocardial trabeculae were detected in thin sections of conventionally fixed material (Fig. 2c) and evaluated by morphometrical methods (see Table I). The EL_1-system follows as a continuous sheet the course of the endocardium thus surrounding the complete outer surface of the trabeculum (Fig. 2b and c, EL_1). The EL_2-system is in close contact to the sarcolemma of myocardial cells (Fig. 2b and c, EL_2). But comparing the expansion of the intercellular space (Fig. 2a, hatched area) between single myocardial cells (Fig. 2a, white areas) with the two-dimensional pattern of the EL_2-system (Fig. 2b, EL_2) reveals clear differences in the topographic appearance. The EL_2-system exclusively invades wide clefts (Fig. 2c, arrow) and is absent in narrow ones (Fig. 2c, arrow-head), *i.e.* large parts of the sarcolemma are devoid of an external lamina. Morphometric data (Table I) demonstrate that the EL_2-system covers althogether 41.1% (SD ± 7.43) of the myocardial cell surface. The extension of the external EL_1-system beneath endocardial cells was not evaluated quantitatively.

2. Histochemistry

Heart muscle cells prepared for the visualization of Ca^{2+}-binding sites in different fixation solutions containing 5 mM, 10 mM or 25 mM Ca^{2+} regularly exhibit numerous small electron-dense deposits along the entire sarcolemma (Fig. 3). A distinct influence of the Ca^{2+}-concentration during fixation and post-treatment exists in so far as both, number and size of the deposits increase with rising Ca^{2+}-content of the medium, *i.e.* best results are obtained with 25 mM Ca^{2+} (Fig. 3a and b). The electron-dense deposits are arranged at the cell surface in more or less regular distances of about 30–40 nm and can be easily dissolved in water. In contrast to myocardial cells other cell types also present in trabeculae such as endocardial cells (Fig. 3c), white blood cells, and fibroblasts always show a negative reaction. The deposits are of characteristic shape with a flat face attached to the external surface of the sarcolemma and a convex face at the opposite site. This can be concluded from thin sections gently poststained with uranyl acetate in 70% ethanol to avoid complete dissolution of the deposits (Fig. 3c, arrows).

X-ray microanalysis demonstrates that calcium is the main element forming the deposits (Fig. 3d and e), whereas calcium in other compartments (myoplasm, intercellular space) is largely lacking (Fig. 3d and f). This is also in agreement with control experiments using Ca^{2+}-free (0.01 mM Ca^{2+}) or EGTA-containing incubation media.

3. Cryopreparations

Quick-freezing of fresh myocardial tissue in liquid propane results in a reliable quality of morphological preservation within a peripheral region of 10–20 µm thickness (Fig. 2d). Main cell organelles such as mitochondria are distinctly visible by the electron-transparent appearance of the membrane systems after staining with uranyl acetate

Table I.

Direction of sectioning	Number of cells	Measured cell-membrane [µm]	% Covered with external lamina (El_2)
longitudinal	26	1445	30.9
longitudinal	24	1447	35.7
longitudinal	15	206	46.6
cross	86	584	38.3
cross	12	86	44.4
cross	159	1285	50.8
	322	5053	$\bar{x} = 41.1\%$ $s = 7.43$

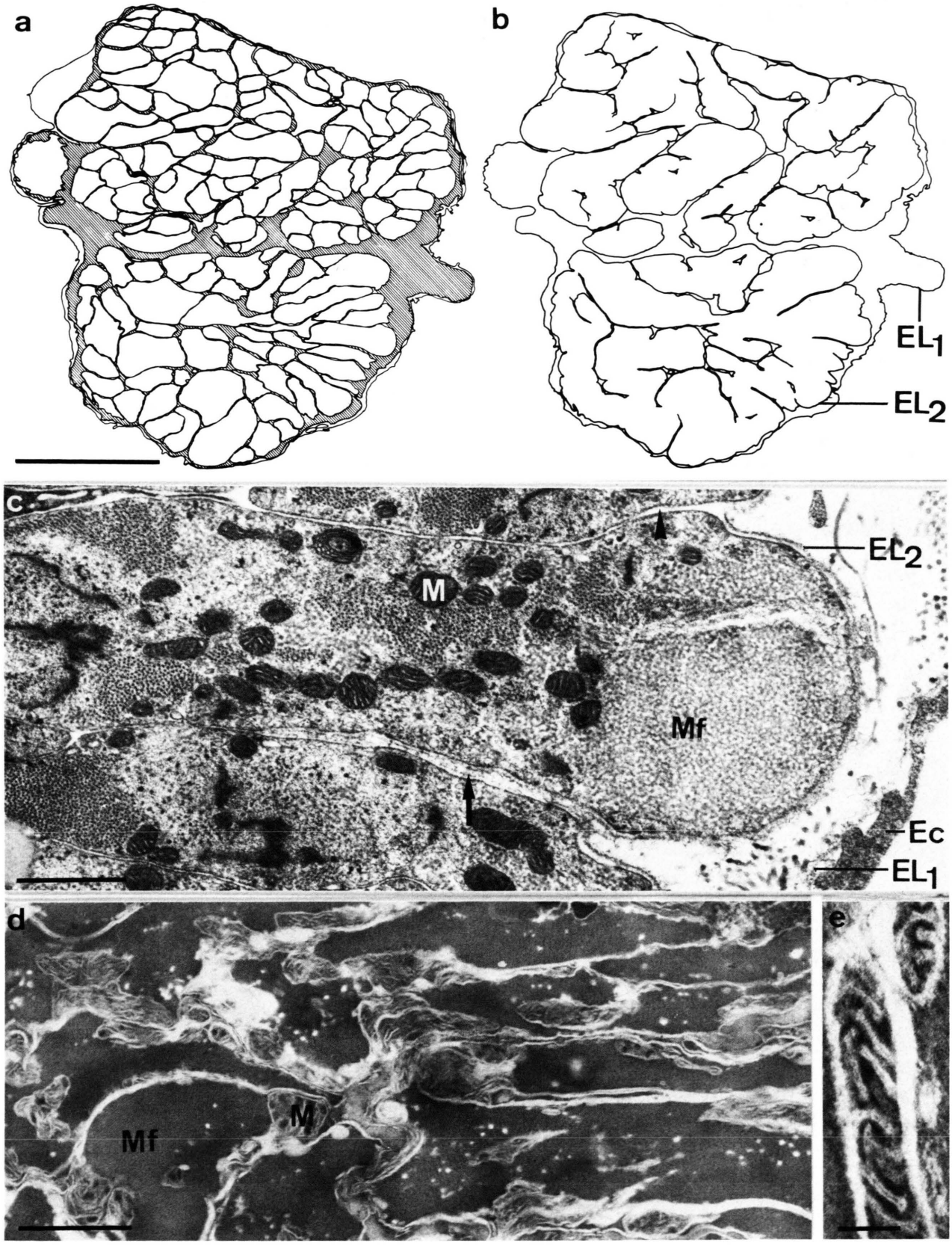

Fig. 2

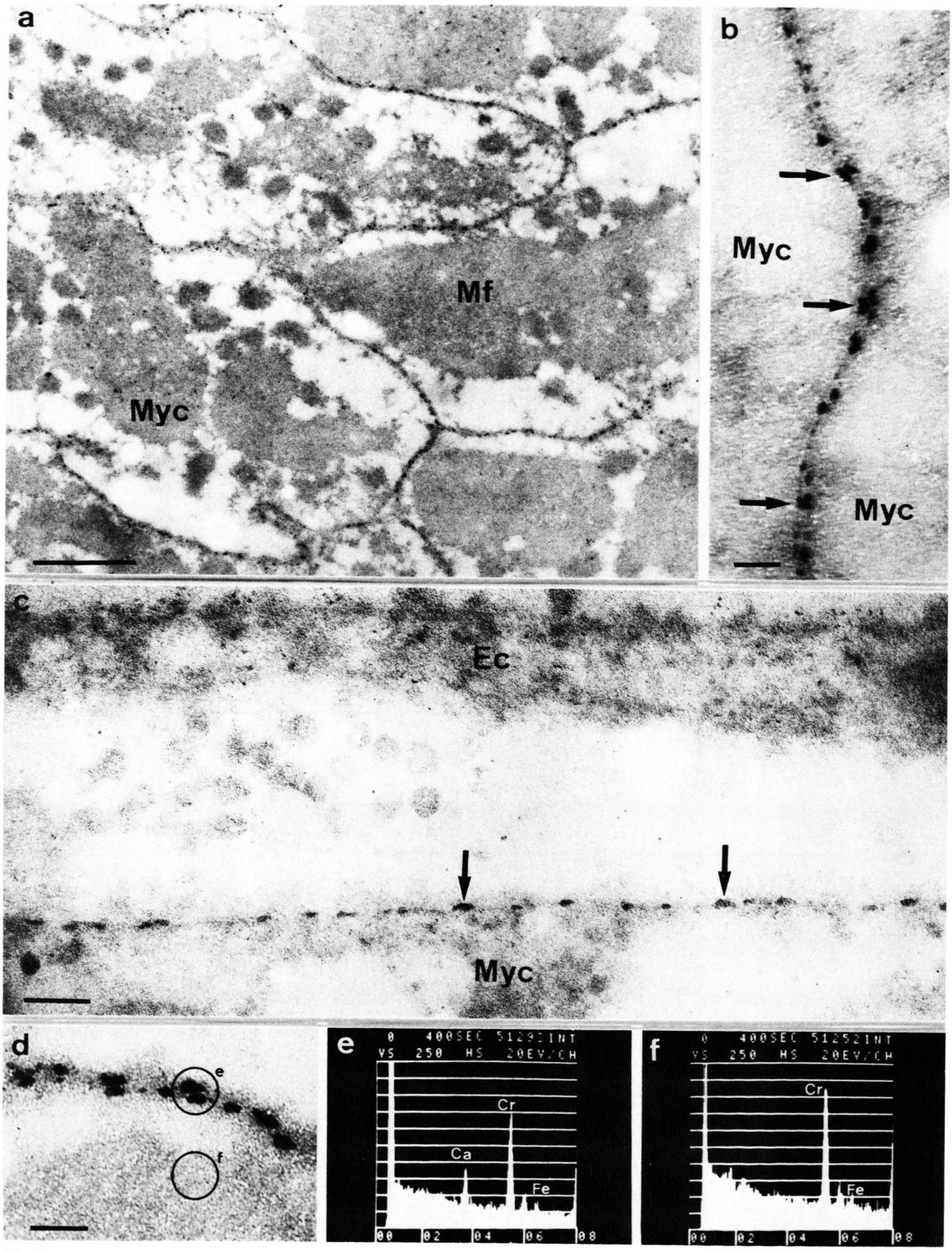
a
Mf
Myc
b
Myc
Myc
c
Ec
Myc
d
e
f
e
0 400SEC 5129INT
VS 250 HS 20EV/CH
Cr
Ca
Fe
00 02 04 06 08
f
0 400SEC 51252INT
VS 250 HS 20EV/CH
Cr
Fe
00 02 04 06 08

Fig. 3

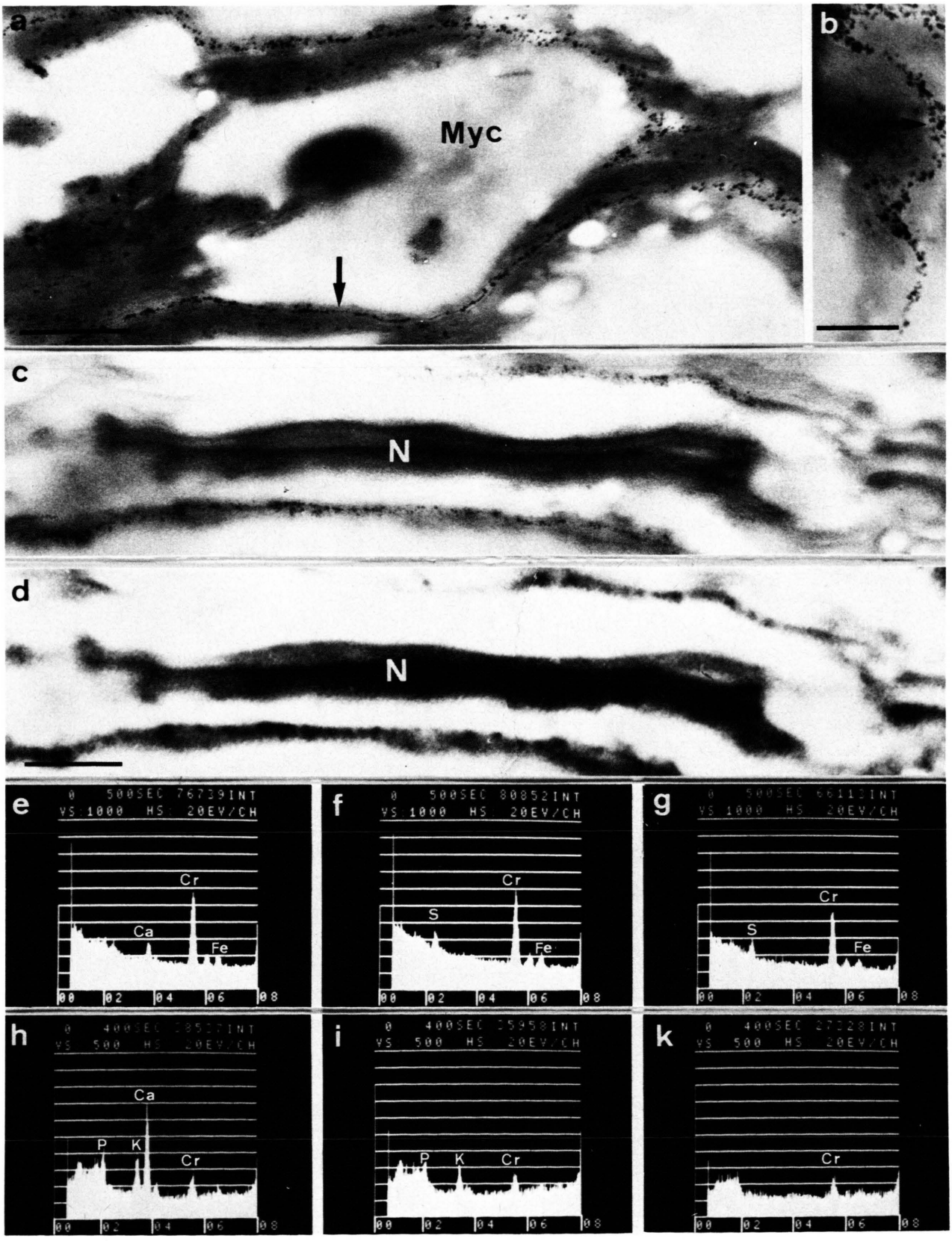

Fig. 4

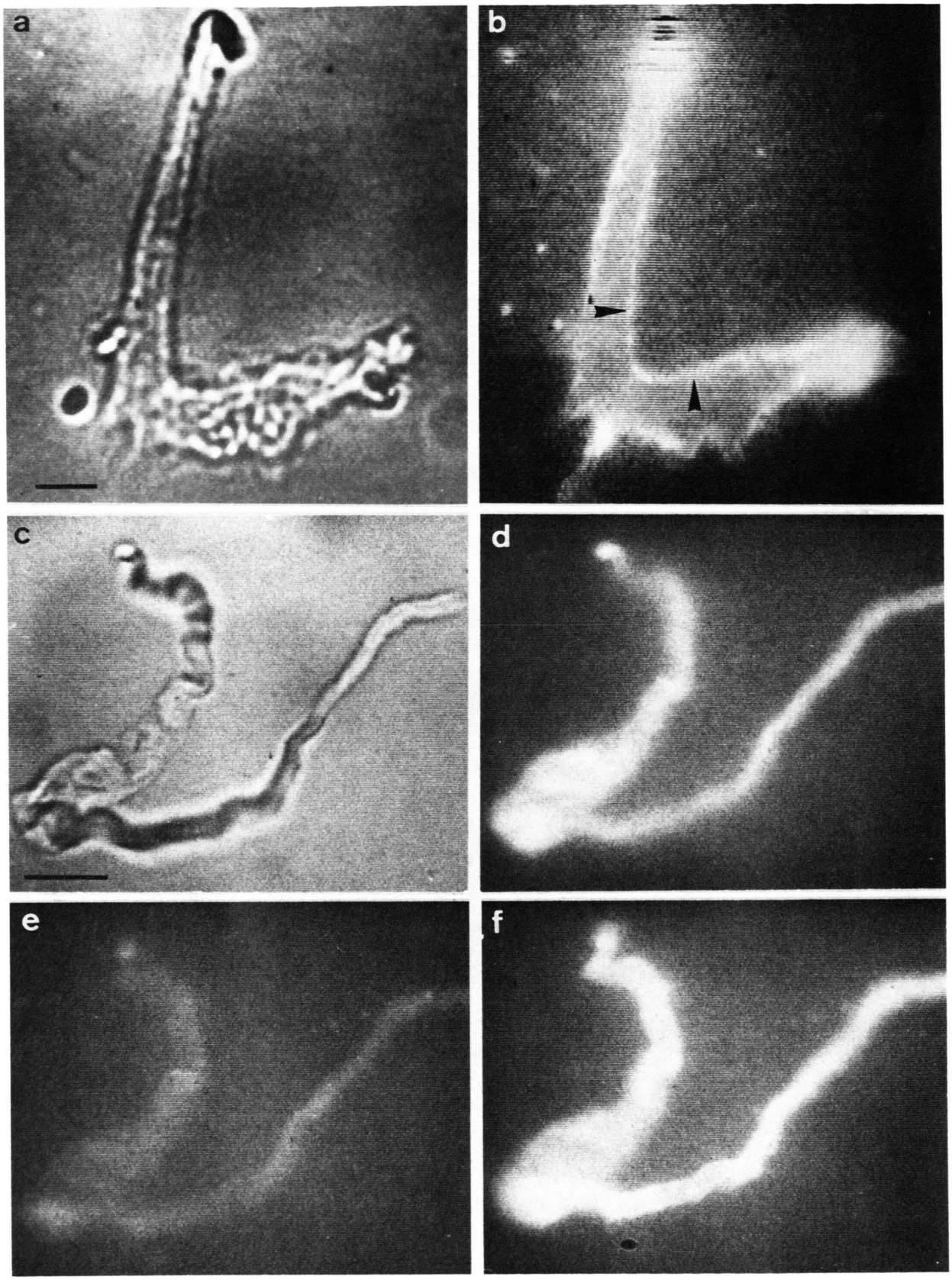

Fig. 5

solution (Fig. 2e). In unstained sections rows of electron-dense deposits at the cell periphery represent the most prominent structures clearly exceeding all other cell constituents in contrast (Fig. 4a and b, arrows). They measure 16.6 nm in diameter (SD ± 5; $n = 50$) and are attached to the sarcolemma. A comparison of thin sections photographed under conventional transmission (TEM, Fig. 4c) and scanning transmission conditions (STEM, Fig. 4d) demonstrates the possibility to visualize the deposits with the STEM-technique and hence to apply X-ray microanalysis (Fig. 4e–k). Sections shortly floated on water before they were mounted on grids deliver a distinct calcium-peak derived from spot analysis of single deposits (Fig. 4e), whereas the cytoplasm (Fig. 4f) and the intercellular space (Fig. 4g) are devoid of detectable amounts of calcium. Sections mounted without any contact to water yield diagrams with increased calcium-peaks and, in addition, significant amounts of potassium and phosphorus (Fig. 4h). Under these conditions potassium and, to a lower extent, phosphorus, are also present in the cytoplasm (Fig. 4i) but not in the intercellular space (Fig. 4k).

4. Fluorescence mircoscopy

Single cells obtained from bullfrog atrium by treatment with trypsin and collagenase (see material and methods) are spindle-shaped or slightly branched and measure 2–10 µm in diameter and 200–400 µm in length (Fig. 5a and c). They can be stained with CTC as a fluorescent probe for membrane-bound Ca^{2+}. The brightness of the resulting CTC-fluorescence signal depends on both, the CTC- and Ca^{2+}-concentration in the incubation medium. A strong fluorescence is obtained with 250 µM CTC and 2 mM Ca^{2+} in Ringer's solution (Fig. 5b), whereas cells treated with 250 µM CTC and 0.01 mM Ca^{2+} show a rather weak fluorescence. Similar results are gained with varying CTC-concentrations at constant Ca^{2+} values. Regardless of changes in intensity, a distinct fluorescence signal always follows to course of the sarcolemma (Fig. 5b, arrow-heads).

Fig. 2. Different morphological aspects of myocardial tissue. a, b) Drawings of a cross-sectioned trabeculum demonstrating a) the expansion of the extracellular space (hatched area) and b) the course of two systems of external laminas (El_1, El_2). El_1 follows the endocardial layer of cells surrounding the trabeculum, El_2 covers parts of the myocardial cell surface. Scale: 10 µm. c) Electron micrograph of a cross-sectioned trabeculum. The El_2-system covers parts of the cell membrane invading into wide clefts (arrow) and lacking within narrow clefts (arrow-head). Ec, endocardial cell. Scale: 0.5 µm. d, e) Cross-sections of cryofixed, freeze-dried tissue poststained with uranyl acetate and lead citrate. Unit membranes show a negative contrast (e). M, mitochondria; Mf, myofibrils. Scale: d) 1 µm, e) 0.1 µm.

Fig. 3. Myocardial tissue showing decoration of Ca^{2+}-binding sites (arrows) after fixation in the presence of 25 mM Ca^{2+}. a) Survey of a cross-section; myocardial cells (Myc) are completely surrounded by electron-dense deposits. Mf, myofibril. Scale: 1 µm. b) Electron-dense deposits (arrows) on the surface of two neighbouring myocardial cells (Myc). Scale: 0.1 µm. c) Ca^{2+}-binding sites present at the membrane of myocardial cells (arrows) but lacking at the surface of endocardial cells (Ec). Scale 0.1 µm. d) Electron-dense deposits used for X-ray microanalysis. Circles (e) and (f) mark the places of X-ray microprobes. Scale: 0.1 µm. e) X-ray spectrum of electron-dense deposits (circle e in d); Ca is detectable in significant amounts. Cr and Fe result from the equipment and not from the probe. f) X-ray spectrum of myoplasm, (circle f in d). The microprobe reveals no Ca.

Fig. 4. Cross-section of cryofixed and freeze-dried tissue, unstained. a, b, c) Transmission electron micrographs demonstrating electron-dense deposits at the cell surface (arrows). Myc, myocardial cell, N, nucleus. Scale: a) 0.5 µm, b) 0.25 µm, c) 0.5 µm. d) Scanning electron micrograph of the same region as shown in c) N, nucleus. e–g) X-ray spectra of a section floated on water before analysis. e) X-ray spectrum of an electron-dense deposit demonstrating the presence of Ca in significant amounts. f) X-ray spectrum of adjacent myoplasm. g) X-ray spectrum of the extracellular space. h–k) X-ray spectra of a section without contact to water before analysis. h) X-ray spectrum of an electron-dense deposit demonstrating the presence of Ca, K and P in significant amounts. i) X-ray spectrum of adjacent myoplasm with P and K. h) X-ray spectrum of the extracellular space.

Fig. 5. Light microscopy of isolated living cells monitored with an image intensification system. a) Bright field image. Scale: 10 µm. b) Fluorescence image of the same cell, stained in 250 µm CTC and 2 mM Ca^{2+}; the cell membrane is visible as a distinct line (arrow-heads). c–f) Experiment with La^{3+} (200 µM). c) Bright field image. Scale: 15 µm. d) Fluorescence image of the same cell, stained in 250 µM CTC and 10^{-5} M Ca^{2+}. e) Solution exchange with 2 mM Ca^{2+} and with 200 µM La^{3+} leads to an obvious decrease in fluorescence. f) Recovery of fluorescence in 2 mM Ca^{2+} without La^{3+} (for explanation see text).

The CTC-Ca^{2+}-fluorescence is inhibited by lanthanum (Fig. 5c–f). Application of a solution containing 2 mM Ca^{2+} and 200 μM La^{3+} to a myocardial cell stained previously with 0.01 mM Ca^{2+} and 250 μM CTC (Fig. 5d) causes a rapid decrease in fluorescence intensity until the signal is nearly vanished (Fig. 5e). Substitution of La^{3+} by a solution containing exclusively 2 mM Ca^{2+} causes recovery of fluorescence (Fig. 5f). This demonstrates that substitution of Ca^{2+} bound to the sarcolemma by La^{3+} is reversible. However, reversibility is only observed if treatment with La^{3+} does not exceed 5 min.

Discussion

Both, the internal and external faces of the plasma membrane are involved in Ca^{2+}-regulation. Binding sites for Ca^{2+} at the internal face were detected histochemically in a variety of tissues and single cells, *e.g.* insect intestine [12], nerves [21–23], amphibian glial cells [24], insect oocytes [25], electrocytes of electrophorus [26], root tip cells [27], cellular slime molds [28], human platelets [29], liver hybrid cells [30], ciliates [31, 32] and amebas [33, 34]. The ability of the plasma membrane to adsorb and release free cytoplasmic Ca^{2+} is of general significance for the control of contractility and cell motility.

Binding sites for Ca^{2+} at the external cell surface are mostly restricted to the existence of negatively charged groups bound to sulphated or phosphorylated sugar components of the glycocalyx [35–39]. In heart muscle cells, the glycocalix is composed of two layers [13]: (i) a surface coat of 20 nm thickness in close contact to the sarcolemma and (ii) an external lamina of 30 nm thickness bordering the interstitial space. The surface coat and external lamina are separate entities. In bullfrog myocardial cells the external lamina (EL_2) covers only 41% of the sarcolemmal surface (see Table I).

All three methods used in this investigation to localize Ca^{2+} and Ca^{2+}-binding sites revealed the surface coat to be the most important compartment for extracellular Ca^{2+}-exchange. This confirms and extends earlier observations, in which extracellular Ca^{2+}-binding sites at the sarcolemma were indirectly detected by the application of La^{3+} [3, 41–43]. However, as La^{3+} exhibits a higher affinity to Ca^{2+}-binding sites than Ca^{2+} itself [2], such experiments are less conclusive than the direct localization of Ca^{2+} by means of cryofixation and freeze-drying (Fig. 4) or by CTC-fluorescence (Fig. 5).

The cryotechnique succeeds in Ca^{2+}-localization under approximate *in vivo*-conditions. Since the pattern of Ca^{2+}-deposits along the sarcolemma in cryofixed specimes is very similar to that determined by the method of Oschman and Wall [12], it seems reasonable to assume that the Ca^{2+}-binding sites demonstrated histochemically are also occupied by Ca^{2+} in living cells.

The demonstration of membrane-bound Ca^{2+} in myocardial cells by CTC as a fluorescent probe is in agreement with observations on other tissues [44–49]. The possibility to displace external Ca^{2+} by La^{3+} (Fig. 5) indicates that the exchangeable Ca^{2+} is bound superficially [42] as already shown in similar experiments with amebas [40]. A significant correlation between the fluorescence intensity of isolated cells on the one hand and the Ca^{2+}-concentration in the perfusing medium on the other hand strongly suggests a participation of the myocardial surface coat in Ca^{2+}-accumulation and release.

The chemical nature of Ca^{2+}-binding sites in the bullfrog myocardial sarcolemma is still obscure. Howse *et al.* [50] as well as Gross and Challice [51] pointed to the anionic nature of the surface coat which is especially rich in sialic acid [42, 52]. Sialic acid is able to bind Ca^{2+}, thereby affecting the physiological properties of the sarcolemma [42, 8]. It should be noted, however, that sialic acid as a common constituent of the glycocalix in a variety of species [38] has not been identified in amphibian myocardial sarcolemma.

Although the functional significance of externally bound Ca^{2+} is not well understood in detail, a wide range of cellular activities is affected by extracellular Ca^{2+}. According to Langer [53] Ca^{2+}-influx from sarcolemmal binding-sites is of major importance in the control of myocardial contractility, *i.e.* membrane-bound Ca^{2+} is involved in excitation-contraction coupling. In amphibian myocardium a Ca^{2+}-release from internal stores does not seem to be important. But Ca^{2+} originating from external sites may act as direct activator of myofilaments. Moreover, Ca^{2+}-binding to the cell surface seems to be a prerequisite for structural integrity of the glycocalix which in turn is important for maintenance of selective membrane permeabilities [42]. When the Ca^{2+}-level of the perfusion-medium is

reduced to a very low level by use of chelating agents, the cardiac action potential is extremely prolonged [54] and the kinetics of the slow inward channel are distinctly delayed [55]. A "stabilizing" effect of external Ca^{2+} on the cell membrane of heart muscle and nerve is well established [56, 57]. The effect was interpreted in terms of an adsorption of Ca^{2+} to the external surface of the membrane which produces a local hyperpolarization and a shift of the current-voltage relations for sodium and potassium to more positive potentials. Observations on amebas [37, 39, 58] have shown that extracellular Ca^{2+} is also necessary to maintain membrane permeability at physiological levels and to provide controlled locomotion and electrical activity in protozoa. In summary, extracellular Ca^{2+}-binding and release constitutes a possible mechanism for the basic control of a number of regulatory processes on the cellular level.

Acknowledgements

The authors wish to thank Dr. C. Achenbach for reading the manuscript and Frl. U. Spies for technical assistance. The investigation was supported by a grant of the Deutsche Forschungsgemeinschaft and a fellowship of the Konrad-Adenauer-Stiftung.

[1] G. A. Langer, Circ. Res. **15,** 393–405 (1964).
[2] W. G. Sandborn and G. A. Langer, J. Gen. Physiol. **56,** 191–217 (1970).
[3] G. A. Langer and J. S. Frank, J. Cell Biol. **54,** 441–455 (1972).
[4] M. J. Legato and G. A. Langer, J. Cell Biol. **41,** 401–423 (1969).
[5] S. Takeo, P. Duke, G. M. L. Taam, P. K. Singal, and N. S. Dhalla, Can. J. Physiol. Pharmacol. **57,** 496–503 (1979).
[6] N. C. Morcos and A. L. Jacobson, Can. J. Physiol. Pharmacol. **57,** 529–534 (1979).
[7] K. D. Philipson, D. M. Bers, A. Y. Nishimoto, and G. A. Langer, Am. J. Physiol. **238,** H373–H378 (1980).
[8] M. P. Matsukubo, P. K. Singal, and N. S. Dhalla, Basic Res. Cardiol. **76,** 16–28 (1981).
[9] I. Inoue, K. Miyama, and Y. Kobatake, Cell Struct. Funct. **3,** 305–311 (1978).
[10] D. M. Bers and G. A. Langer, Am. J. Physiol. **237,** H332–H341 (1979).
[11] A. Fabiato and F. Fabiato, Ann. N.Y. Acad. Sci. **307,** 491–522 (1978).
[12] J. Oschman and B. J. Wall, J. Cell Biol. **55,** 58–73, (1972).
[13] G. A. Langer, Am. J. Physiol. **235,** H461–H468 (1978).
[14] A. J. Dalton, Anat. Rec. **121,** 281 (1955).
[15] K. E. Wohlfarth-Bottermann, Naturwissenschaften **44,** 287 (1957).
[16] A. R. Spurr, J. Ultrastruc. Res. **26,** 31–43 (1969).
[17] K. Zierold, Microscopica Acta **83,** 25–32 (1980).
[18] M. Tarr and J. W. Trank, Experientia **32,** 338–340 (1976).
[19] M. Tarr, J. W. Trank, P. Leiffer, and N. Shepherd, Circ. Res. **45,** 554–559 (1979).
[20] A. H. Caswell and J. D. Hutchison, Biochem. Biophys. Res. Com. **42,** 43–49 (1971).
[21] J. Oschman, T. A. Hall, P. D. Peters, and B. J. Wall, J. Cell Biol. **61,** 156–161 (1974).
[22] D. E. Hillmann and R. Llinás, J. Cell Biol. **61,** 146–155 (1974).
[23] A. F. Boyne, T. P. Bohan, and T. H. Williams, J. Cell Biol. **63,** 780–795 (1974).
[24] P. Gambetti, S. E. Bulkar, A. P. Somlyo, and N. K. Gonatas, J. Cell Biol. **64,** 322–330 (1975).
[25] A. Przelecka and A. Sobota, Cytobiologie **13,** 182–190 (1976).
[26] T. C. de Auraujo Jorge, W. de Souza, and R. D. Machado, J. Cell Sci. **38,** 97–104 (1979).
[27] N. V. Belitser, G. V. Zaalishvili, and N. P. Sytnianskaja, Protoplasma **111,** 63–78 (1982).
[28] C. Chastellier and A. Ryter, Biol. Cell. **43,** 121–128 (1982).
[29] R. J. Skaer, P. D. Peters, and J. P. Emmines, J. Cell Sci. **15,** 679–692 (1974).
[30] W. Larsen, J. Cell Biol. **67,** 801–813 (1975).
[31] H. Plattner, J. Cell Sci. **18,** 257–269 (1975).
[32] G. Fisher, E. S. Kaneshiro, and P. D. Peters, J. Cell Biol. **69,** 429–442 (1976).
[33] A. Sobota, B. Hrebenda, and A. Przelecka, Cytobiol. **15,** 259–265 (1977).
[34] W. Stockem and H. P. Klein, Protoplasma **100,** 33–43 (1979).
[35] H. J. Allen, C. Ault, R. J. Winzler, and J. F. Danielli, J. Cell Biol. **60,** 26–38 (1974).
[36] K. Braatz-Schade and W. Stockem, Z. Zellforsch. **137,** 97–109 (1973).
[37] J.-O. Josefsson, Acta Physiol. Scan. Suppl. **432,** 1–65 (1975).
[38] J. H. Luft, Int. Rev. Cyt. **45,** 291–382 (1976).
[39] W. Stockem, in: Mammalian Cell Membranes (G. A. Jamieson and D. M. Robinson, eds.), **Vol. 5,** pp.151–195, Butterworths, London 1977.
[40] W. Gawlitta, W. Stockem, J. Wehland, and K. Weber, Cell Tiss. Res. **213,** 9–20 (1980).
[41] A. Martinez-Palomo, D. Benitez, and J. Alanis, J. Cell Biol. **58,** 1–10 (1973).
[42] J. S. Frank, G. A. Langer, L. M. Nudd, and K. Seraydarian, Circ. Res. **41,** 702–714 (1977).
[43] E. Weihe, W. Hartschuh, J. Metz, and U. Brühl, Cell Tiss. Res. **178,** 285–302 (1977).
[44] D. E. Chandler and J. A. Williams, J. Cell Biol. **76,** 386–399 (1978).
[45] P. M. Saling and B. T. Storey, J. Cell Biol. **83,** 544–555 (1979).
[46] H. D. Reiss and W. Herth, Protoplasma **97,** 373–377 (1978).
[47] H. D. Reiss and W. Herth, Planta **146,** 615–621 (1979).
[48] S. M. Wolniak, P. K. Hepler, and W. T. Jackson, J. Cell Biol. **87,** 23–32 (1980).

[49] G. Wagner and R. Rossbacher, Planta **149,** 298–305 (1980).
[50] H. D. Howse, V. J. Ferrans, and R. G. Hibbs, J. Mol. Cell. Cardiol. **1,** 157–168 (1970).
[51] D. Gros and C. E. Challice, J. Histochem. Cytochem. **23,** 727–744 (1975).
[52] G. A. Langer, J. S. Frank, and K. D. Philipson, Circ. Res. **49,** 1289–1299 (1981).
[53] G. A. Langer, J. Mol. Cell. Cardiol. **12,** 231–239 (1980).
[54] D. J. Miller and A. Mörchen, J. Gen. Physiol. **71,** 47–67 (1978).
[55] R. Meyer, H. M. Einwächter, and H. G. Haas, in prep.
[56] S. Weidmann, J. Physiol. **129,** 568–582 (1955).
[57] B. Frankenhaeuser and A. L. Hodgkin, J. Physiol. **137,** 218–244 (1957).
[58] K. Braatz-Schade, Acta Protozool. **17,** 163–176 (1978).